

## TROPICAL INFLUENCE ON THE SOUTH PACIFIC DOUBLE JET VARIABILITY

Akio KITO

*Meteorological Research Institute, 1-1, Nagamine, Tsukuba 305*

**Abstract:** An observational and modeling study of the interannual variability of the South Pacific atmospheric circulation is presented. The observed data cover the period 1979–1991. An atmospheric general circulation model (GCM) has been integrated with the observed sea surface temperature (SST) for the period 1970–1989. It is shown that the subtropical jet is positively correlated with the SST anomalies in the central equatorial Pacific. Thus, the jet is directly influenced by the tropical heating. On the other hand, the high latitude jet variability is associated with a wave train through eastern Australia, south-east of New Zealand, West Antarctica and southern South America. It is found from the stationary wave flux analysis that when the SST anomalies in the Indian Ocean are positive, this wave train is formed in a location to weaken the Pacific high latitude jet both in the observed data and in the GCM. The GCM is shown to have a capability to model the interannual variability of the South Pacific double jet forced by the SST variations.

### 1. Introduction

The Southern Hemisphere (SH) circulation is characterized by a mid tropospheric double jet structure in winter in the South Pacific and a semiannual oscillation of sea-level pressure (SLP) in high southern latitudes. The zonal wind at 500 hPa in SH winter has two maxima in the Pacific sector, one around 30°S and the other around 60°S, and only one maximum in the Atlantic/Indian sector. Quasi-stationary eddy fields with zonal wavenumber 1 at 50°–70°S are associated with this zonal asymmetry. XU *et al.* (1990) compared the performance of four spectral general circulation models (GCM) with observations and showed that models have a deficiency in simulating both the double jet and the semiannual oscillation. Higher resolution models tend to more reasonably simulate the SH circulation features (MITCHELL and SENIOR 1989; BOVILLE 1991). KITO *et al.* (1990) showed that the Meteorological Research Institute (MRI) GCM successfully simulated such circulation features.

Although there is a double jet structure in a climatological sense, a large variability exists. Several papers have investigated the variability of the winter-time subtropical jet east of Australia and related it to equatorial convection on various time scales (*e.g.*, KNUTSON and WEICKMANN 1987; NOGUES-PAEGLE and MO 1988). There also are studies concerning the high latitude jet and stationary wave variability (*e.g.*, MEEHL 1987; JAMES 1988), but the relationship between this and tropical heating is inconclusive.

There is little literature which addresses the variability of the South Pacific double jet produced in GCM simulations. In this paper, we focus on interannual variations of the South Pacific double jet in winter produced by a 20-year integration of the MRI GCM with observed sea surface temperatures (SST). The purpose of this paper is twofold: first, to show the model performance in simulating interannual variability of the South Pacific double jet, and second, to see whether they are related to SST variability and tropical heating anomalies. The latter can be analyzed from the GCM output forced by SST which changes interannually as observed in the last 20 years. The observational analyses based on the 13-year (1979–1991) data are shown and simulated results are compared with them.

## 2. Data

Observed data used are the twice-daily global objective analyses by the U.S. National Meteorological Center for the 13 year period 1979–1991. As a proxy for convection, outgoing longwave radiation (OLR) data from the NOAA polar orbiting satellites are also used.

The MRI GCM used in this study is a grid model with a horizontal resolution of  $4^\circ$  latitude and  $5^\circ$  longitude. It has 5 levels in the vertical with a top at 100 hPa. Full physical processes with diurnal as well as seasonal variation of solar insolation are included. A 20.5 year integration has been performed with the prescribed SST from September 1969 to February 1990. The observed SST covers the oceans for  $40^\circ\text{S}$ – $60^\circ\text{N}$ . South of  $40^\circ\text{S}$ , the climatological SST was used. KITOH (1991a, b) describes the interannual variations simulated in this experiment

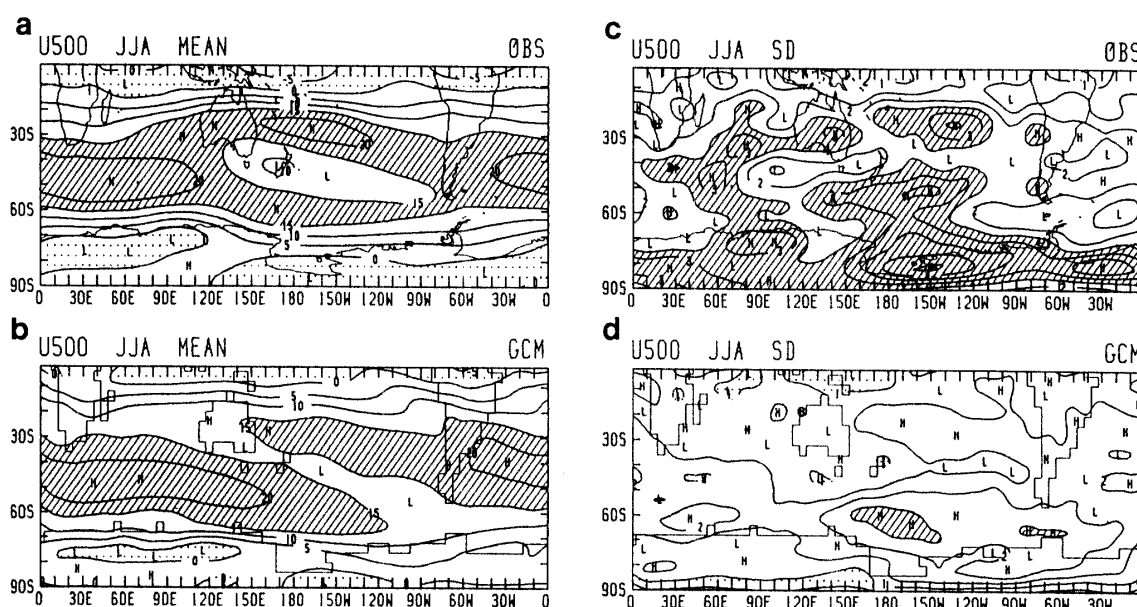


Fig. 1. (a) Observed 13-year mean June–July–August U500. Contour interval is 5 m/s. (b) Simulated 20-year mean June–July–August U500. (c) Standard deviation of the observed seasonal mean U500. Contour interval is 0.5 m/s. (d) Standard deviation of the simulated seasonal mean U500.

in the tropics and the decadal changes of Northern Hemisphere (NH) circulations associated with a meridional shift of the subtropical jet in NH.

Figure 1 shows the observed and simulated zonal wind at 500 hPa (U500) in austral winter (June–July–August) and their interannual standard deviation. The observed climatological (13-year mean) map (Fig. 1a) shows a single jet in the Atlantic and Indian Oceans and a double jet in the Pacific. The lower latitude jet in the Pacific has a maximum in the upper troposphere, while the higher latitude jet is connected with a lower tropospheric core, corresponding to two large meridional temperature gradient regions (KITOH *et al.*, 1990). As shown in Fig. 1c, there is quite a large interannual variation in the Pacific sector. In fact, there are years with a clear double jet structure (*e.g.*, 1989) and years without it (*e.g.*, 1988).

This GCM has already shown reasonable performance of the SH circulations such as the South Pacific double jet in winter and the semiannual oscillation in southern middle-high latitudes (KITOH *et al.*, 1990). The simulated U500 has maxima at 30°S and 66°S and a minimum at 46°S in the Pacific sector in winter (Fig. 1b). Interannual variability of the simulated U500 is the largest in the South Pacific, but is weaker than the observed. This is partly because the GCM has its upper boundary at 100 hPa. The GCM has years both with and without the double jet structure in the Pacific.

### 3. Low Latitude Jet in the Pacific

There are many observational and numerical studies on the relationship between tropical heating and the subtropical jet east of Australia. These studies have emphasized the role of a local Hadley circulation due to the effect of organized latent heat release on subtropical jet acceleration. NOGUES-PAEGLE and Mo (1988) showed that the response of subtropical latitudes to tropical latent heat release is fully established in about 10 days.

Figure 2 shows the observed correlations between the intensity of the South Pacific subtropical jet (U500) and SST, OLR and SLP for the period 1979–1991. Here U500 is the average for the region 180°W–120°W, 36°S–24°S. The SST in the central equatorial Pacific is positively correlated with U500, while the SST in the western Pacific is negatively correlated. Correlations for OLR indicate that more active convection is observed in the central equatorial Pacific, caused by positive SST anomalies. These convection anomalies are responsible for the variability of the subtropical jet. In the upper troposphere, there is an anticyclonic circulation anomaly in the central Pacific just south of the equator with its center around 15°S and a cyclonic anomaly east of New Zealand (40°S), consistent with the wind anomalies. The SLP anomaly pattern is on a global scale with wave number 1 in the tropics, reflecting the SST variation. Height anomalies are baroclinic equatorward of about 20°S and barotropic poleward of this latitude.

Corresponding maps for the GCM are shown in Fig. 3. Simulated subtropical jet variability is also attributed to the central equatorial Pacific SST changes. A dipole heating anomaly pattern is seen over the equator to the east and to the

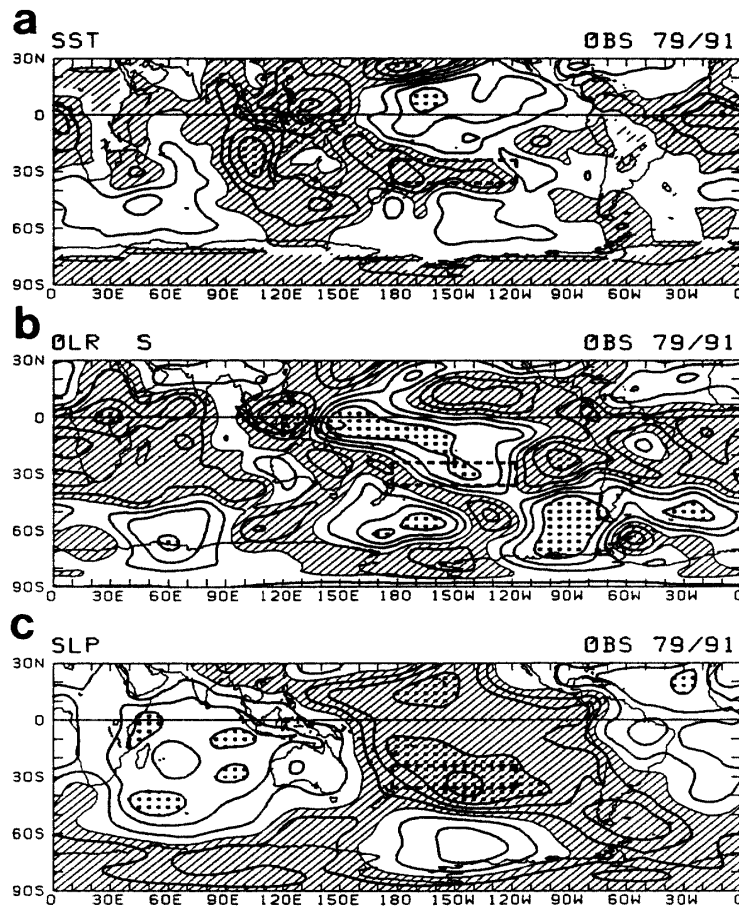


Fig. 2. (a) Observed correlations between  $U500$  at  $180^{\circ}\text{W}$ – $120^{\circ}\text{W}$ ,  $36^{\circ}\text{S}$ – $24^{\circ}\text{S}$  and SST. Observed seasonal (JJA) mean values for 1979–1991 are used. Contour interval is 0.2. Negative values are hatched. Dots indicate that the correlation is significant at the 95% level. (b) As in (a) except for OLR. Positive values are hatched. (c) As in (a) except for SLP.

west of the date line. These equatorial heating anomalies produce upper tropospheric anticyclonic circulation anomalies symmetric about and straddling the equator, accompanied by intensified upper tropospheric westerly anomalies in the subtropics east of Australia. Negative SLP anomalies are simulated to the south of this latitude. This is a simple example of atmospheric responses to equatorial heating anomalies. Thus, the model is successful in simulating interannual variations of the subtropical jet associated with equatorial SST variations in the Pacific.

#### 4. High Latitude Jet in the Pacific

Figure 4 shows the observed correlations for SST, OLR and SLP with the intensity of the high latitude jet ( $180^{\circ}\text{W}$ – $120^{\circ}\text{W}$ ,  $68^{\circ}\text{S}$ – $56^{\circ}\text{S}$ ). Correlations for SLP (Fig. 4c) show a distinct wave train over the South Pacific which seems to emanate from the maritime continent (Indonesia, New Guinea and north of

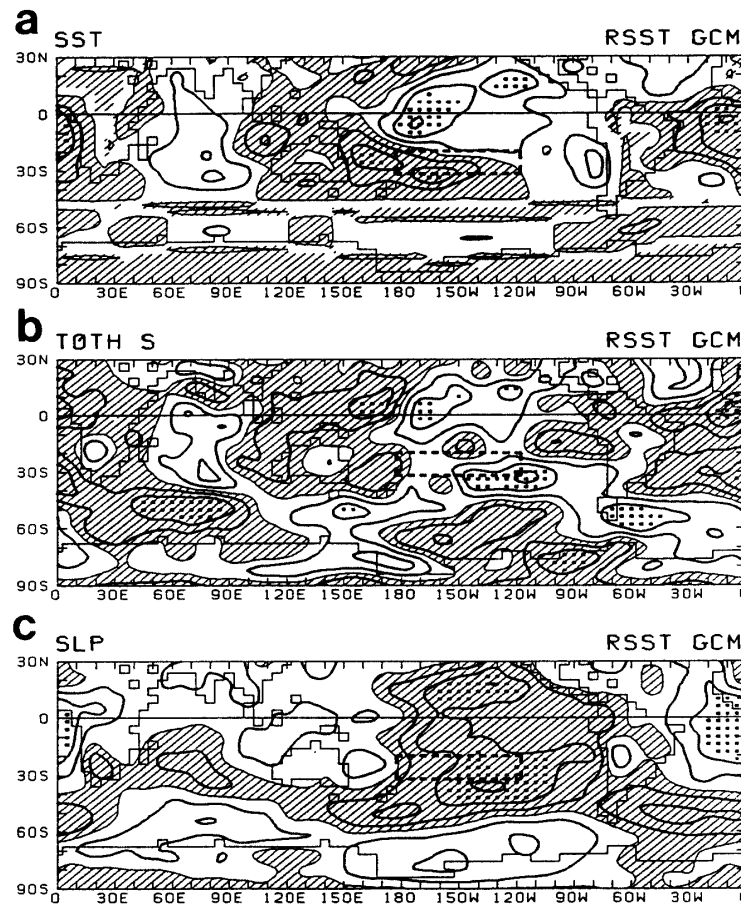


Fig. 3. (a) Simulated correlations between simulated  $U500$  at  $180^{\circ}\text{W}$ – $120^{\circ}\text{W}$ ,  $32^{\circ}\text{S}$ – $20^{\circ}\text{S}$  and SST. (b) As in (a) except for total diabatic heating rate. (c) As in (a) except for SLP.

Australia). In the tropics, SLP anomalies are positive in the eastern Pacific and Indian Ocean, and negative in the western Pacific. These SLP anomalies are common at the time of La Niña (Fig. 4a). Correlations for SST anomalies in the maritime continent are close to zero. Correlations are significantly negative over the tropical Indian Ocean. OLR anomalies are not significant (Fig. 4b), but convections are relatively vigorous in the maritime continent.

The simulated counterparts to Fig. 4 are shown in Fig. 5. Correlations for SLP (Fig. 5c) are more elongated than the observations in the South Pacific, and a north-south seesaw pattern with a node around  $60^{\circ}\text{S}$  is associated with the jet variability. Together with this seesaw pattern, there is a wave train in the South Pacific. Figure 5b is the correlations for the total diabatic heating rate. The total diabatic heating is the sum of latent heat release by condensation, sensible heat flux convergence and net radiational heating. Condensation is the leading term in the total diabatic heating. In fact, a map for precipitation is very similar to Fig. 5b. It is shown that there are positive heating anomalies in the maritime continent in accordance with observations. These heating anomalies are associated with a contrast in SST anomalies between the Indian Ocean and the western

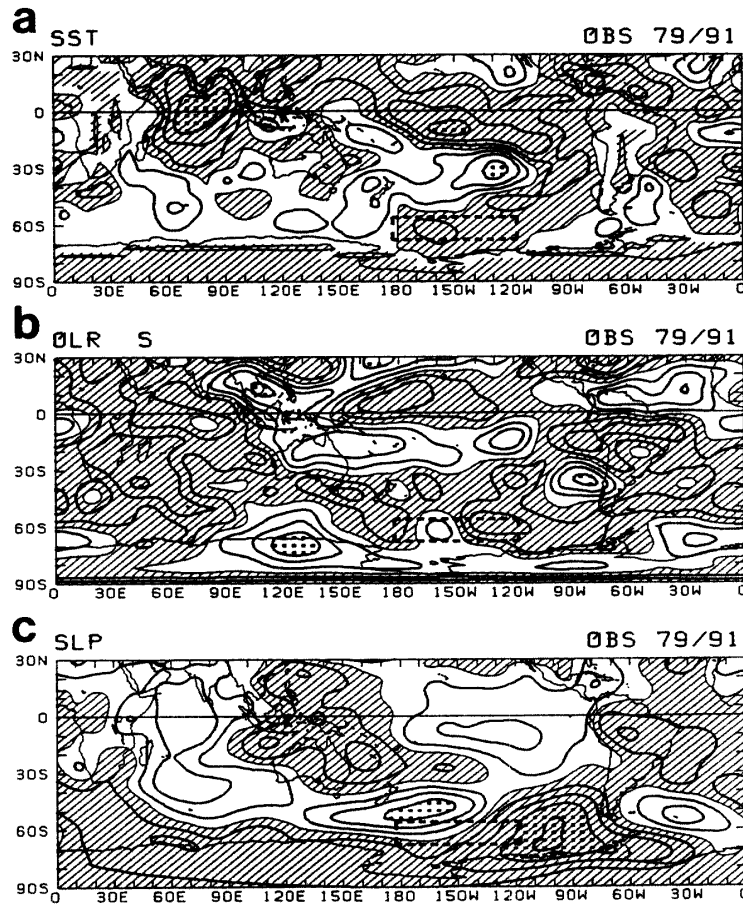


Fig. 4. (a) Observed correlations between  $U_{500}$  at  $180^{\circ}\text{W}$ – $120^{\circ}\text{W}$ ,  $68^{\circ}\text{S}$ – $56^{\circ}\text{S}$  and SST. (b) As in (a) except for OLR. (c) As in (a) except for SLP.

Pacific (Fig. 5a). Precipitation anomalies in the South Pacific near the reference area are the result of circulation changes. It is noted that both the observed and simulated correlation maps for SST have significantly negative regions in the Indian Ocean.

Figures 4c and 5c suggest Rossby-like propagation of stationary waves. There are plenty of works on the propagation of wave activity and on the interaction between waves and the mean flow. PLUMB (1985) derived the stationary wave flux to diagnose the three-dimensional propagation of planetary-scale stationary wave activity. KAROLY *et al.* (1989) showed that in the SH winter there is a major source of stationary wave activity flux over the Indian Ocean with zonal propagation south of Australia and then equatorward propagation east of New Zealand. Recently, YANG and GUTOWSKI (1994) compared the stationary wave activity flux simulated by two GCMs with the NMC analyses. They showed that the models have difficulty in simulating both the strength and the direction of stationary wave activity flux in the SH.

Figure 6 shows the observed composite map of the 500 hPa geopotential height ( $Z_{500}$ ) anomalies and horizontal stationary wave flux defined as:

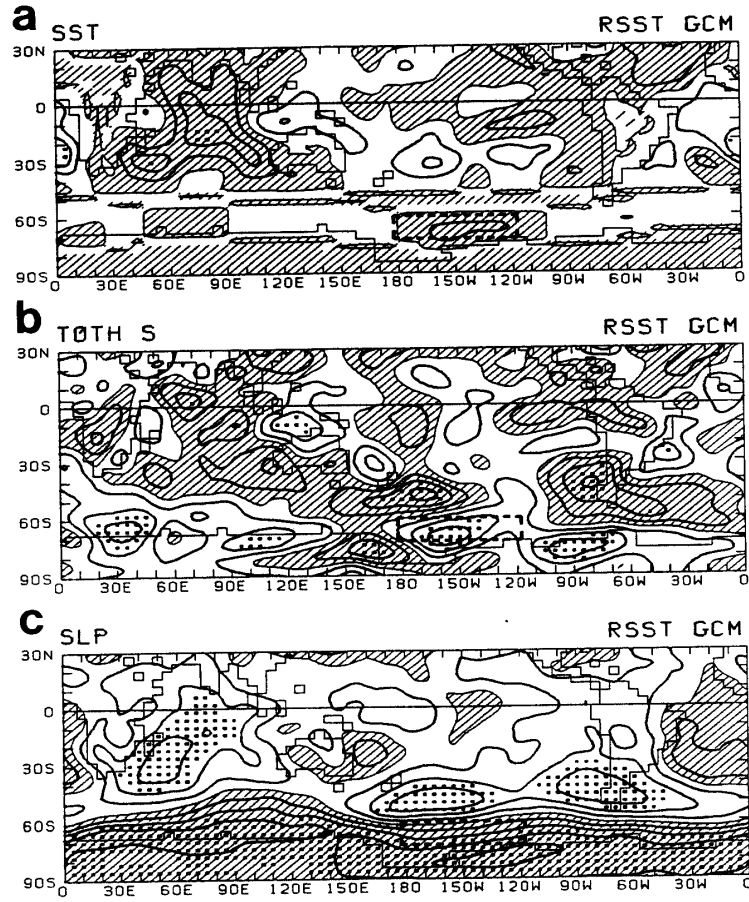


Fig. 5. (a) Simulated correlations between  $U_{500}$  at  $180^{\circ}\text{W}$ – $120^{\circ}\text{W}$ ,  $72^{\circ}\text{S}$ – $60^{\circ}\text{S}$  and SST. (b) As in (a) except for total diabatic heating rate. (c) As in (a) except for SLP.

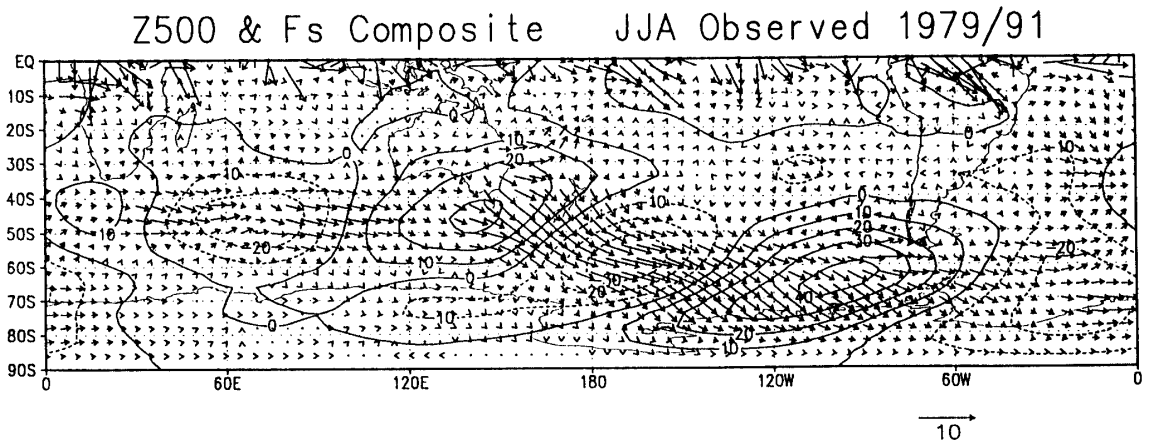


Fig. 6. Observed composite of the geopotential height anomaly and stationary wave activity flux at 500 hPa.

$$\begin{aligned}
 (F_{\lambda}, F_{\phi}) = & \cos \phi (v^{*2} - (2 \Omega a \sin 2\phi)^{-1} \partial(v^* \Phi^*) / \partial \lambda, \\
 & -u^* v^* + (2 \Omega a \sin 2\phi)^{-1} \partial(u^* \Phi^*) / \partial \lambda), \quad (1)
 \end{aligned}$$

where  $u$  and  $v$  are geostrophic winds and  $*$  is deviation from the zonal mean. Three years' data, from 1980, 1987 and 1990, are composited for a weak high latitude westerlies case. The height anomaly pattern is almost identical to that for SLP (Fig. 4c), and, considering the polarity of the composite, anomalies are quasi-barotropic in middle and high latitudes. There is an anomalous stationary eddy forcing into the South Pacific from the South Indian Ocean and Australia, causing an anomalous low around  $60^{\circ}\text{S}$ ,  $180^{\circ}$ – $150^{\circ}\text{W}$ . Climatologically, there is a stationary wave number 1 pattern with a ridge in the South Pacific, due to the Antarctic topography (KITOH *et al.*, 1990). Existence of this stationary wave is essential in forming the high latitude part of the double jet in the South Pacific. The anomalous stationary eddy forcing contributes to split (reinforce) the stationary wave number 1 high pressure in the South Pacific and to weaken (strengthen) the high latitude jet.

AOKI *et al.* (1986) showed by lagged correlations of 5-day mean Z500 that stronger westerlies in  $50^{\circ}$ – $60^{\circ}\text{S}$  in the South Pacific are related to a wave train from Australia and have a close relationship with the activity of the subtropical high in the western North Pacific. They also showed eastward movement of a highly correlated area from the Indian Ocean to the southeastern coast of Australia in 15 days. This may be connected with eastward wave flux of the seasonal mean anomaly composite in the South Indian Ocean shown in Fig. 6. A direct tropical influence on stationary eddy activity flux is not clear, as the flux in the Indian Ocean is stronger. But there is a southeastward flux from eastern Australia, corresponding to SLP anomalies shown in Fig. 4c (negative correlation region around  $160^{\circ}\text{E}$ ,  $20^{\circ}\text{S}$ ).

The simulated composite of the stationary wave flux is shown in Fig. 7. The simulated Z500 anomalies and thus the wave activity flux are weaker than the observed. There is a wave flux from the Indian Ocean and Australia into the South Pacific. The flux then moves toward South America. In this simulated composite, contributions of stationary wave flux into the South Pacific from possible tropical origin are more evident than in the observed composite. The resultant wave train contributes to weaken the westerlies in the high latitude

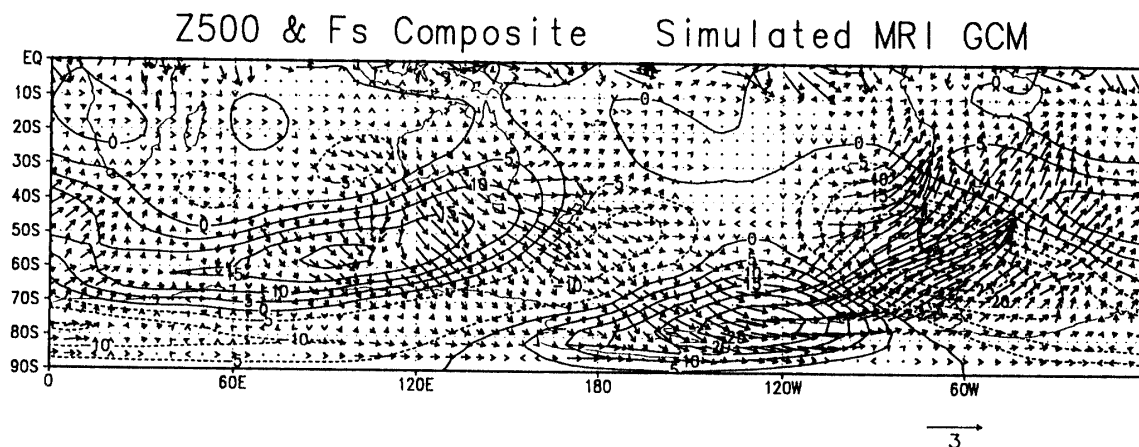


Fig. 7. As in Fig. 6 except for the simulation.



South Pacific in this composite.

The forcing mechanisms for the stationary wave activity include orographic forcing, thermal forcing, instabilities of the jet and transient eddies. KAROLY *et al.* (1989) and YANG and GUTOWSKI (1994) suggest that the nonlinear interaction with transient eddies is a major, but not the only, source of the SH stationary waves. There also are observational studies that the low frequency SH variability is governed by transient eddy momentum activity. KIDSON (1988) showed that the leading low frequency variability mode in the SH with a period greater than 50 days is associated with a barotropic fluctuation between subtropical and high latitude jets with a three-wave pattern at midlatitudes. This mode is preceded a few days earlier by eddy momentum flux changes. SHIOTANI (1990) showed a close relationship between the double jet structure and the activity of stationary planetary wave and transient eddy activity using daily 500 hPa geopotential height data. He showed that when the height in the polar region is low and the double jet is evident, transient eddy activity along the Antarctic is vigorous in the South Pacific sector and maintains the high latitude jet. Both KIDSON (1988) and SHIOTANI (1990) showed the active role of the eddy momentum flux and the negligible role of the eddy heat flux on the high latitude jet variability.

Thus model simulations of stationary wave flux activity in the SH may be sensitive to their simulation of transient eddies in the upper troposphere (YANG and GUTOWSKI 1994). To investigate the role of eddy activity in high latitude jet maintenance, the momentum budget is analyzed using daily GCM outputs. Figure 8 shows the latitudinal distribution of correlation coefficients between high latitude jet intensity and four terms of the momentum budget equation for the zonal acceleration  $\partial[\bar{u}]/\partial t$  at 300 hPa, *i.e.*,

$f [\bar{v}]$	Coriolis torque,
$-(a \cos^2\phi)^{-1} \partial\{[\bar{u}'v'] \cos^2\phi\}/\partial\phi$	transient eddy momentum flux convergence,
$-(a \cos^2\phi)^{-1} \partial\{[\bar{u}^*v^*] \cos^2\phi\}/\partial\phi$	stationary eddy momentum flux convergence,
$-(a \cos^2\phi)^{-1} \partial\{[\bar{u}][\bar{v}] \cos^2\phi\}/\partial\phi$	zonal mean circulation term,

where  $\bar{\quad}$  is time mean,  $'$  is deviation from time mean,  $[\quad]$  is zonal mean and  $*$  is deviation from zonal mean.

It is shown that the acceleration of the high latitude jet is associated mainly with the transient eddy flux convergence. The Coriolis torque is the main balancing term to the transient eddy flux convergence. This model result is in accord with previous observational studies. Geographically, we find that the southward transient eddy momentum flux in the South Pacific region around 50°–60°S contributes to accelerate the westerlies south of 60°S and decelerate them around 30°–40°S. The latter can be seen in Fig. 8 where the transient eddy momentum flux term is opposite between high latitudes and middle latitudes.

Figure 9a shows the correlations between the transient eddy momentum flux convergence in the 68°S–60°S latitude belt and the 500 hPa height field. The

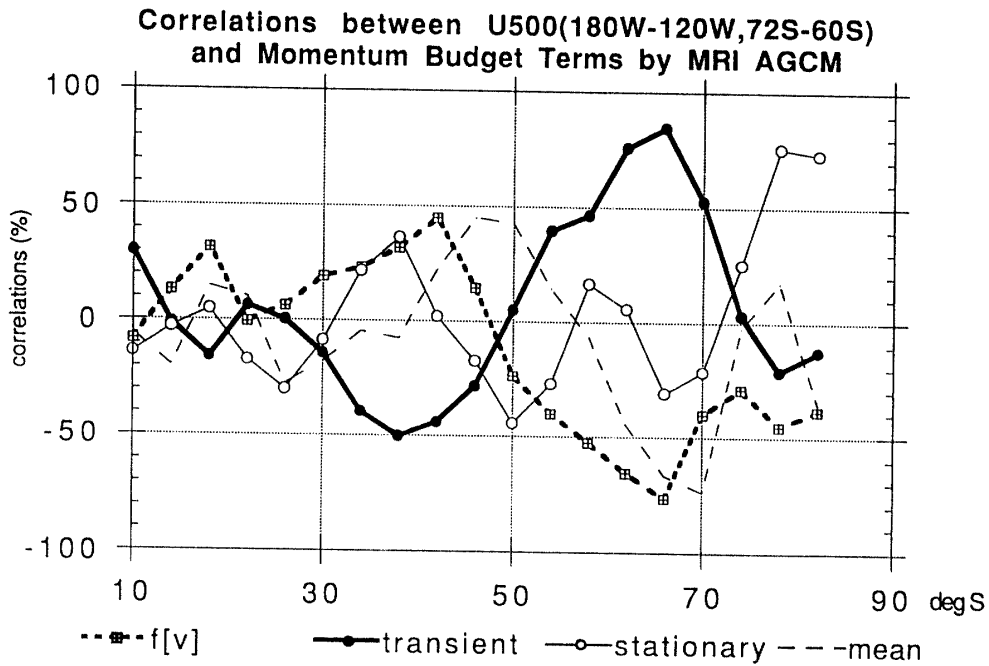


Fig. 8. Correlations between high latitude jet intensity (zonal wind at 500 hPa averaged 180°W–120°W, 72°S–60°S) and various terms of the momentum budget equation at 300 hPa. The thin solid line is the Coriolis term; thick solid line is the transient eddy momentum flux; thick dashed line is the stationary eddy momentum flux; thin dashed line is the zonal mean motion.

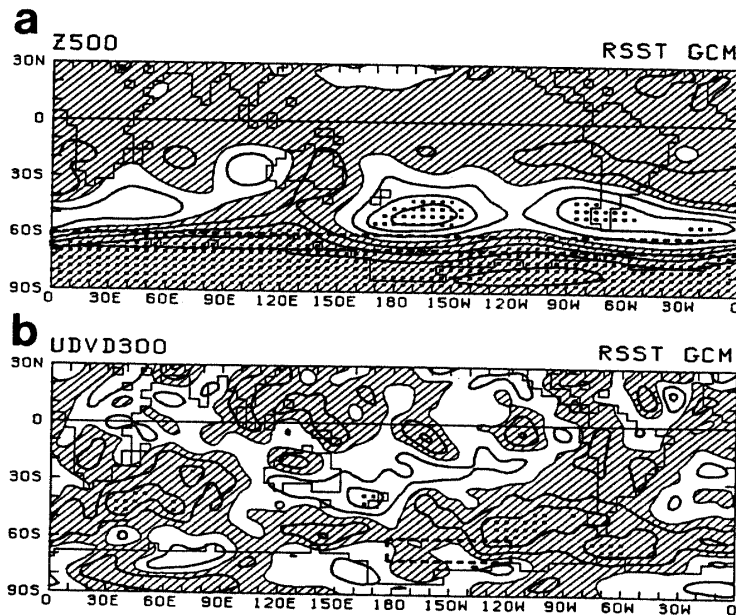


Fig. 9. (a) Correlations between the transient eddy momentum flux convergence at 68°S–60°S and the 500 hPa height field. (b) Correlations between high latitude jet intensity (zonal wind at 500 hPa averaged 180°W–120°W, 72°S–60°S) and the transient eddy momentum flux at 300 hPa.

stationary eddy field reveals a feature which appears when the high latitude jet is strong in the South Pacific (see Fig. 5c and Fig. 7c). Figure 9b shows the geographical region of strong transient eddy momentum flux associated with the high latitude jet variability. It is shown that the storm track regions in the Indian Ocean and in the South Pacific are the major regions which are related to the acceleration of the jet. It is also shown that the area with significant correlations in the South Pacific is located downstream of the reference region, suggesting a secondary role of the transient eddies on the stationary eddy formation compared to the thermal forcing, probably from low latitudes. Correlation analysis (not shown) also indicates a significant relationship between this transient eddy momentum flux in the South Pacific and the circulations in the maritime continent. These results suggest that the stationary wave related to the high latitude jet variability is mainly forced by tropical thermal forcing, and supported by transient eddy activity. These results should be checked with more GCM experiments with anomalous forcings.

## 5. Summary

An observational and modeling study of the interannual variability of the South Pacific atmospheric circulation is presented. The low latitude part of the jet is directly influenced by the tropical heating anomaly around the date line along the equator, associated with the SST anomalies in the central equatorial Pacific. The high latitude jet variability is associated with a wave train over the South Pacific. This wave train is related to anomalous heating and resultant circulation changes in the maritime continent and may be related to the tropical SST anomaly contrast between the Indian Ocean and the western Pacific. Analyses for the stationary wave activity flux and the transient eddy momentum flux suggest that the high latitude jet variability is mainly forced by tropical thermal forcing, with support from transient eddy activity.

## References

- AOKI, T., KAWAHARA, M. and YAMADA, S. (1986): 500 mb kôdo-ba ni okeru Kitataiheyô seibu no natsu no a-nettai kôkiatsu to Minami Hankyû no fuyu to no kankei (Relationship in 500 mb geopotential height field between summer subtropical high in the western North Pacific and winter Southern Hemisphere). *Kishô-chô Kenkyû Jihô* (J. Meteorol. Res.), **38**, 203–208.
- BOVILLE, B. A. (1991): Sensitivity of simulated climate to model resolution. *J. Clim.*, **4**, 469–485.
- JAMES, I. N. (1988): On the forcing of planetary-scale Rossby waves by Antarctica. *Q. J. R. Meteorol. Soc.*, **114**, 619–637.
- KAROLY, D. J., PLUMB, R. A. and TING, M. (1989): Examples of the horizontal propagation of quasi-stationary waves. *J. Atmos. Sci.*, **46**, 2802–2811.
- KIDSON, J. W. (1988): Interannual variations in the Southern Hemisphere circulation. *J. Clim.*, **1**, 1177–1198.
- KITOH, A. (1991a): Interannual variations in an atmospheric GCM forced by the 1970–1989 SST. Part I: Response of the tropical atmosphere. *J. Meteorol. Soc. Jpn.*, **69**, 251–269.
- KITOH, A. (1991b): Interannual variations in an atmospheric GCM forced by the 1970–1989 SST. Part II: Low-frequency variability of the wintertime Northern Hemisphere extratropics. *J. Meteorol. Soc. Jpn.*, **69**, 271–291.

- KITOH, A., YAMAZAKI, K. and TOKIOKA, T. (1990): The double-jet and semi-annual oscillations in the Southern Hemisphere simulated by the Meteorological Research Institute general circulation model. *J. Meteorol. Soc. Jpn.*, **68**, 251–264.
- KNUTSON, T. R. and WEICKMANN, K. M. (1987): 30–60 day atmospheric oscillations: Composite life cycles of convection and circulation anomalies. *Mon. Weather Rev.*, **115**, 1407–1436.
- MEEHL, G. A. (1987): The annual cycle and interannual variability in the tropical Pacific and Indian Ocean regions. *Mon. Weather Rev.*, **115**, 27–50.
- MITCHELL, J. F. B. and SENIOR, C. A. (1989): The antarctic winter simulations with climatological and reduced sea-ice extents. *Q. J. R. Meteorol. Soc.*, **115**, 225–246.
- NOGUES-PAEGLE, J. and MO, K. C. (1988): Transient response of the Southern Hemisphere subtropical jet to tropical forcing. *J. Atmos. Sci.*, **45**, 1493–1508.
- PLUMB, R. A. (1985): On the three-dimensional propagation of stationary waves. *J. Atmos. Sci.*, **42**, 217–229.
- SHIOTANI, M. (1990): Low-frequency variations of the zonal mean state of the Southern Hemisphere troposphere. *J. Meteorol. Soc. Jpn.*, **68**, 461–471.
- XU, J.-S., VON STORCH, H. and VAN LOON, H. (1990): The performance of four spectral GCM in the Southern Hemisphere: The January and July climatology and the semiannual wave. *J. Clim.*, **3**, 53–70.
- YANG, S. and GUTOWSKI, W. J., JR. (1994): GCM simulations of the three-dimensional propagation of stationary waves. *J. Clim.*, **7**, 414–433.

*(Received December 9, 1993; Revised manuscript received July 29, 1994)*